Physics-informed online estimation of compliance with Gelsight sensor

Abstract— **Softness perception is essential for tactile sensing applications, including robotic manipulation, medical diagnostics, and virtual reality. Traditional approaches to estimate material compliance are either data-driven, requiring extensive datasets, or physics-based, which often lack robustness to variations in object geometry. Here, we present a hybrid method combining machine learning with physics-informed constraints to improve the accuracy and physical plausibility of Young's modulus estimation in real time. Using tactile images from a Gelsight sensor and an estimation informed by Hertzian contact mechanics, we show in this paper that our system can predict stiffness at 15 Hz. Tested on a set of real fruits, the method demonstrated reliable performance with a Mean Absolute Relative Error of 25.6%, highlighting its potential for dynamic remote sensing applications.**

I. INTRODUCTION

When interacting with objects, humans naturally perceive properties such as friction or compliance through their sense of touch, specifically by using fingertip deformation [6]. However, replicating this capability in tele-robotics where an operator control a manipulator at a distance remains a significant challenge, specially in softness perception [7]. The remote users usually rely on vision only, and when tactile properties are rendered, it is generally only as a kinesthetic cue using force-feedback devices [5].

Existing approaches to estimate softness are categorized into data-driven and physics-based methods. Data-driven methods rely on large datasets to train models to map sensory inputs to material properties [10]. These methods are very effective in specific scenarios, such as tumor detection [4] or harvesting ripe fruits [3]. However, they often suffer from a lack of generalization to unseen objects, particularly over a wide range of material types. Physics-based methods on the other hand, aim to model the mechanical interactions [8]. They are very interpretable and robust; however, they often involve computationally intensive simulations, which makes real-time applications impossible.

In this paper, we proposed a new method that combines both approaches, integrating machine learning with physics-informed constraints to improve the speed and accuracy of the estimation while maintaining physical plausibility. To predict the stiffness in real time, the model used high-resolution tactile images from a Gelsight sensor to extract deformation features, along with a Hertzian contact mechanics estimate. The results suggest that this method can achieve a reliable estimation at 15 Hz suitable for highly dynamic and unstructured environments.

II. MATERIALS & METHODS

A. Experimental platform

We mounted a two-finger parallel jaw gripper on the ALOHA right arm [1]. The fingertips are equipped with gelsight wedge sensors [9] on both sides. In the experiment, we assumed symmetry between fingers so we acquired data from only the left finger. The sensor outputs an RGB image with 88 black markers as shown in figure 1B. The normal force was measured through a gauge (HX711) embedded in the right finger and the gripper width was acquired from the aloha control software 1D.

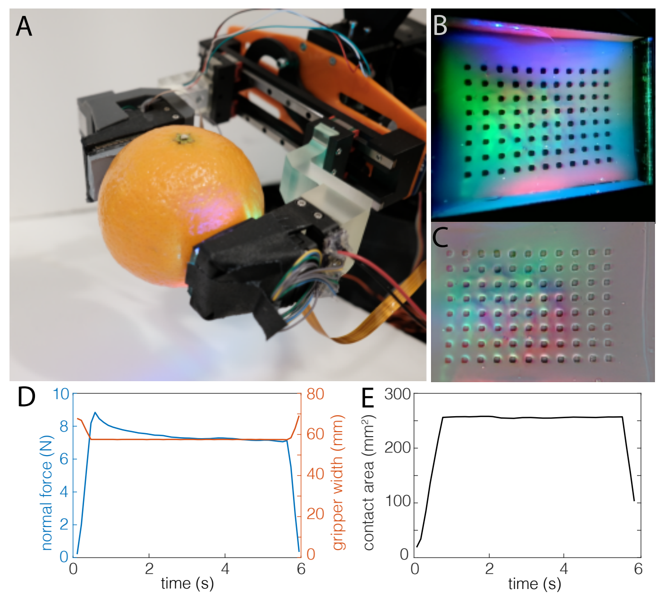

Fig. 1. **A.** Tactile gripper grasping a real orange. **B.** Raw image from the Gelsight sensor. **C.** Processed difference image. **D.** Normal force, gripper width and contact area acquired on a typical trial. **E.** Contact area measured from the tactile image.

B. Young's modulus estimation

The model that we used for the Young's modulus estimation has been trained on a diverse dataset of 285 objects, with Young's moduli ranging from 5.0 kPa to 250 MPa [2]. The model takes the tactile images from the Gelsight sensor, the normal force f_n, the gripper width w along with one Young's modulus estimate from the Hertzian analytical model.

Hertzian contact theory models the penetration depth from the stress and strain distribution (1). The estimated equivalent Young's modulus E^* is a function of the Young's modulus and poisson's ratio ν of both the sensor and the object.

$$\begin{cases} E^* = \left(\dfrac{1-\nu_s^2}{E_s} + \dfrac{1-\nu_o^2}{E_o}\right)^{-1} \\ d(t) = \dfrac{1-\nu_s^2}{E_s}\left(\dfrac{3\pi^2 {E^*}^2 f_n(t)\,(w(t)-w(t_c))}{32\,a_c(t)^2}\right)^{1/3} \end{cases} \quad (1)$$

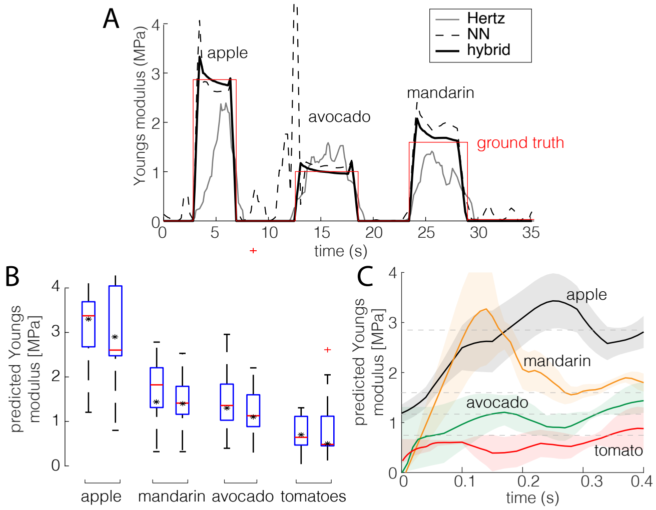

Fig. 2. **A.** Temporal prediction of the Young's moduli when successively grasping an apple, an avocado and a mandarin for three methods (Hertzian analytical model, Neural Network alone, our hybrid method). The red line indicates the ground truth. **B.** Predicted Young's moduli of four fruits. The ground truth is indicated by the asterisks. **C.** Estimated Young's moduli as a function of time from the first contact.

where t_c is the instant of first contact with the object, d the deformation of the sensor and a_c the contact area determined by masking the depth images with a threshold of 0.1 mm (figure 1E).

III. RESULTS

To assess the generalizability of stiffness estimation, we tested the model on four different couple of fruits: two apples, two mandarins, two avocados and two tomatoes. The Young's moduli of the fruits were computed from the Shore A using the following equation:

$$E = 0.1614e^6 \ \exp(0.0541\,\mathrm{shore\,A}) \qquad (2)$$

Young's moduli were evaluated for each fruit and are reported in Fig. 2B with asterisks. The fruits were selected to cover different material properties and stiffness values ranging from 0.5 to 3.3 MPa. For reference, the Young's modulus of our silicone sensor is 0.275 MPa.

We achieved 8 successive grasps of the fruits and estimated the Young's moduli with three methods (Hertzian analytical model, Neural Network alone, our hybrid method). A typical online estimation of the compliance is plotted in Figure 2A along with the ground truth.

Figure 2B highlights the predicted Young's moduli for each fruit with our hybrid method, the ground truth values are denoted by the asterisks. The results indicate that the model consistently tracks the ground truth values across different stiffness ranges, with slightly larger standard deviations for stiffer objects such as the apple.

Figure 2C provides temporal dynamics of Young's modulus estimation from the very first contact. The predictions stabilize quickly after the initial contact, demonstrating the model's ability to adapt to changing grasp conditions in real time. Notably, the temporal curves for softer fruits like tomato and avocado exhibit more precise predictions for a normal force as low as 0.3 N.

We evaluated the predictions against the ground truth for different methods by computing the absolute relative differences as follow:

$$\text{Relative MAE} = \frac{1}{N}\sum \frac{\left|E_{GT\,i} - \hat{E}_i\right|}{E_{GT\,i}} \qquad (3)$$

Methods	Relative MAE	Time to cvg
Hertzian analytical model	40.9%	0.77 s
NN without analytical estimate	34.5%	0.19 s
Hybrid (our method)	25.6%	0.24 s

TABLE I
ACCURACY OF THE YOUNG'S MODULUS ESTIMATION

Table I summarizes the estimation accuracy and time to converge achieved by various methods: the Hertzian contact model and the trained neural network with and without the use of the analytical estimate. The neural network alone outperforms a strictly analytical method, but the best performance is achieved when the two methods are combined, giving error of only 25.6%. This underscores the value of incorporating physics-informed inputs into machine learning models.

IV. DISCUSSION

Our results demonstrate that integrating physics-informed constraints significantly enhances the accuracy of machine-learning-based compliance estimation. Incorporating Hertzian contact mechanics into the model improved prediction accuracy by almost 10% compared to purely data-driven approaches.

However, the model faced challenges in distinguishing small stiffness differences, particularly among harder objects with moduli farther from that of the Gelsight sensor. This limitation underscores the importance of sensor-material compatibility and suggests opportunities for optimization, such as incorporating adaptive algorithms or extending the sensor's sensitivity range by adding layers of different stiffnesses for example. We also observed slower performance in converging to the ground truth for the hardest fruits. Interestingly, for the mandarin, the model shows an overestimation of the Young's modulus before converging to the ground truth. This can be explained by the fact that the mandarin is a highly heterogeneous fruit, the sensor deformation first encodes the fruit skin and then the pulp.

Future work will focus on providing the model's output as tactile feedback to a remote user. This application would enable enhanced teleoperation experiences, where users could intuitively perceive material properties through haptic feedback. Such advancements could facilitate remote robotic control in fields like surgical robotics, where real-time tactile information is critical.

ACKNOWLEDGMENT

This study was funded by [removed for double-blind review purpose]

REFERENCES

[1] J. Aldaco, T. Armstrong, R. Baruch, J. Bingham, S. Chan, K. Draper, D. Dwibedi, C. Finn, P. Florence, S. Goodrich, et al. Aloha 2: An enhanced low-cost hardware for bimanual teleoperation. *arXiv preprint arXiv:2405.02292*, 2024.

[2] M. Burgess and J. Zhao. Learning object compliance via young's modulus from single grasps with camera-based tactile sensors. *arXiv preprint arXiv:2406.15304*, 2024.

[3] F. E. Erukainure, V. Parque, M. A. Hassan, and A. M. FathEl-Bab. Estimating the stiffness of kiwifruit based on the fusion of instantaneous tactile sensor data and machine learning schemes. *Computers and Electronics in Agriculture*, 201:107289, 2022.

[4] M. Li, A. Faragasso, J. Konstantinova, V. Aminzadeh, L. D. Seneviratne, P. Dasgupta, and K. Althoefer. A novel tumor localization method using haptic palpation based on soft tissue probing data. In *2014 IEEE International Conference on Robotics and Automation (ICRA)*, pages 4188–4193. IEEE, 2014.

[5] D. Prattichizzo, F. Chinello, C. Pacchierotti, and M. Malvezzi. Towards wearability in fingertip haptics: a 3-dof wearable device for cutaneous force feedback. *IEEE Transactions on Haptics*, 6(4):506–516, 2013.

[6] M. A. Srinivasan and R. H. LaMotte. Tactual discrimination of softness. *Journal of neurophysiology*, 73(1):88–101, 1995.

[7] C. J. Stabile, D. J. Levine, G. M. Iyer, C. Majidi, and K. T. Turner. The role of stiffness in versatile robotic grasping. *IEEE Robotics and Automation Letters*, 7(2):4733–4740, 2022.

[8] Z. Su, J. A. Fishel, T. Yamamoto, and G. E. Loeb. Use of tactile feedback to control exploratory movements to characterize object compliance. *Frontiers in neurorobotics*, 6, 2012.

[9] S. Wang, Y. She, B. Romero, and E. Adelson. Gelsight wedge: Measuring high-resolution 3d contact geometry with a compact robot finger. In *2021 IEEE International Conference on Robotics and Automation (ICRA)*, pages 6468–6475. IEEE, 2021.

[10] W. Yuan, C. Zhu, A. Owens, M. A. Srinivasan, and E. H. Adelson. Shape-independent hardness estimation using deep learning and a gelsight tactile sensor. In *2017 IEEE International Conference on Robotics and Automation (ICRA)*, pages 951–958. IEEE, 2017.